

Non-perturbative renormalization group calculation of the quasi-particle velocity and the dielectric function of graphene

Carsten Bauer, Andreas Rückriegel, Anand Sharma, and Peter Kopietz
*Institut für Theoretische Physik, Universität Frankfurt,
 Max-von-Laue Strasse 1, 60438 Frankfurt, Germany*
 (Dated: June 29, 2015)

Using a non-perturbative functional renormalization group approach we calculate the renormalized quasi-particle velocity $v(k)$ and the static dielectric function $\epsilon(k)$ of suspended graphene as functions of an external momentum k . Our numerical result for $v(k)$ can be fitted by $v(k)/v_F = A + B \ln(\Lambda_0/k)$, where v_F is the bare Fermi velocity, Λ_0 is an ultraviolet cutoff, and $A = 1.37$, $B = 0.51$ for the physically relevant value ($e^2/v_F = 2.2$) of the coupling constant. In contrast to calculations based on the static random-phase approximation, we find that $\epsilon(k)$ approaches unity for $k \rightarrow 0$. Our result for $v(k)$ agrees very well with a recent measurement by Elias *et al.* [Nat. Phys. **7**, 701 (2011)].

PACS numbers: 81.05.ue, 11.10.Hi, 71.10.-w

At low energies the physical properties of graphene are dominated by the Dirac points where the energy dispersion vanishes linearly. In this regime many-body effects become important and can be measured experimentally [1]. In view of the great interest in graphene both for fundamental research and applied physics, it is important to gain a thorough understanding of correlation effects. Of particular interest is the renormalization of the Fermi velocity at the Dirac points by long-range Coulomb interactions, which has been observed experimentally in suspended graphene using cyclotron resonance [2], in ARPES measurements of quasi-freestanding graphene on SiC [3], and in graphene on hexagonal boron nitride (hBN) [4]. Early one-loop renormalization group (RG) calculations [5] predicted a logarithmic enhancement of the renormalized Fermi velocity,

$$v_\Lambda/v_F = 1 + (\alpha/4) \ln(\Lambda_0/\Lambda) + \mathcal{O}(\alpha^2), \quad (1)$$

where Λ is the infrared cutoff introduced in the RG procedure, Λ_0 is an ultraviolet cutoff of the order of the inverse lattice spacing, $v_F = 10^6$ m/s is the bare Fermi velocity, and $\alpha = e^2/v_F$ is the relevant dimensionless coupling constant. Because for graphene suspended in vacuum $\alpha \approx 2.2$ is rather large, perturbative RG calculations are not expected to be quantitatively accurate.

In this work, we use a functional renormalization group (FRG) approach [6, 7] to derive non-perturbative RG flow equations for the cutoff- and momentum-dependent velocity $v_\Lambda(k)$ and the static dielectric function $\epsilon_\Lambda(q)$ of suspended graphene. Since we are interested in the RG flow of momentum-dependent *functions*, the field theoretical RG is not sufficient, because with this method one can only keep track of a finite set of coupling *constants*. We show here that this problem can be solved within the FRG formalism [6, 7]; specifically, we derive two coupled integro-differential equations for the cutoff-dependent functions $v_\Lambda(k)$ and $\epsilon_\Lambda(q)$ which are non-perturbative in α and self-consistently describe the interplay between self-energy and screening effects.

Our starting point is the following effective Hamiltonian describing the low-energy physics of graphene,

$$\mathcal{H} = \sum_p \int_{\mathbf{k}} \hat{\psi}_p^\dagger(\mathbf{k}) (v_p \boldsymbol{\sigma} \cdot \mathbf{k}) \hat{\psi}_p(\mathbf{k}) + \frac{1}{2} \int_{\mathbf{q}} f_{\mathbf{q}} \hat{\rho}_{-\mathbf{q}} \hat{\rho}_{\mathbf{q}}, \quad (2)$$

where $p = \pm$ labels the two Dirac points of the underlying tight-binding model on a honeycomb lattice, $v_p = pv_F$ is the bare Fermi velocity at Dirac point p , and $\hat{\psi}_p(\mathbf{k})$ are two-component fermionic field operators whose components are associated with the two sublattices of the honeycomb lattice. The two-component vector $\boldsymbol{\sigma} = (\sigma^x, \sigma^y)$ contains Pauli matrices acting on sublattice space, and two-dimensional momentum integrations are denoted by $\int_{\mathbf{k}} = \int \frac{d^2k}{(2\pi)^2}$. The interaction in Eq. (2) is specified in terms of the Fourier transform $f_{\mathbf{q}} = 2\pi e^2/|\mathbf{q}|$ of the Coulomb interaction and the Fourier components of the density operators, $\hat{\rho}_{\mathbf{q}} = \sum_p \int_{\mathbf{k}} \hat{\psi}_p^\dagger(\mathbf{k}) \hat{\psi}_p(\mathbf{k} + \mathbf{q})$. For simplicity, we consider a given spin projection and suppress the spin label. We shall insert the spin-degeneracy $N_s = 2$ of the electrons in Eq. (10) below.

To derive FRG flow equations, we introduce a cutoff Λ which inhibits the propagation of electrons with momenta $|\mathbf{k}| < \Lambda$. For our purpose it is sufficient to work with a sharp momentum cutoff. The regularized free propagator is then $G_{p,\Lambda}^0(K) = \Theta(k - \Lambda) [i\omega - v_p \boldsymbol{\sigma} \cdot \mathbf{k}]^{-1}$, where the label $K = (\mathbf{k}, i\omega)$ represents momentum \mathbf{k} and fermionic Matsubara frequency $i\omega$. At some large initial cutoff Λ_0 of the order of the inverse lattice spacing the regularized Euclidean action of our system is

$$S_{\Lambda_0}[\psi, \phi] = - \sum_p \int_K \psi_p^\dagger(K) [G_{p,\Lambda_0}^0(K)]^{-1} \psi_p(K) + \frac{1}{2} \int_Q [f_{\mathbf{q}}^{-1} \phi(-Q) \phi(Q) + 2i\rho(-Q) \phi(Q)], \quad (3)$$

where $\psi_p(K)$ is a two-component Grassmann field and we have used a Hubbard-Stratonovich transformation to represent the Coulomb interaction in terms of a scalar field $\phi(Q)$ which couples to the Fourier components

$\rho(Q) = \sum_p \int_K \psi_p^\dagger(K) \psi_p(K+Q)$ of the density. The integration symbols are $\int_K = \int_{\mathbf{k}} \int \frac{d\omega}{2\pi}$ and $\int_Q = \int_{\mathbf{q}} \int \frac{d\bar{\omega}}{2\pi}$. Here $Q = (\mathbf{q}, i\bar{\omega})$, where $i\bar{\omega}$ is a bosonic Matsubara frequency. It is now straightforward to write down a formally exact flow equation for the generating functional $\Gamma_\Lambda[\psi, \phi]$ of the irreducible vertices describing their change as we reduce the infrared cutoff $\Lambda_0 \rightarrow \Lambda$. By construction for $\Lambda \rightarrow 0$ the flowing vertices reduce to the exact irreducible vertices of our original Hamiltonian (2). As usual, we obtain an approximate solution of this functional flow equation by working with a truncated form of $\Gamma_\Lambda[\psi, \phi]$. For our purpose, the following truncation is sufficient,

$$\begin{aligned} \Gamma_\Lambda[\psi, \phi] = & - \sum_p \int_K \psi_p^\dagger(K) G_{p,\Lambda}^{-1}(K) \psi_p(K) \\ & + \frac{1}{2} \int_Q \phi(-Q) F_\Lambda^{-1}(Q) \phi(Q) \\ & + \sum_{p,s} \int_K \int_Q \Gamma_{p,\Lambda}^s(K, Q) \bar{\psi}_p^s(K+Q) \psi_p^s(K) \phi(Q), \end{aligned} \quad (4)$$

where in the last term $s = A, B$ is the sublattice label and $\psi_p^s(K)$, $\bar{\psi}_p^s(K)$ are the sublattice components of $\psi_p(K)$ and the adjoint spinor $\psi_p^\dagger(K)$. It is convenient to express the renormalized fermionic and bosonic propaga-

tors in terms of the corresponding self-energies as usual, $G_{p,\Lambda}^{-1}(K) = [G_{p,\Lambda}^0(K)]^{-1} - \Sigma_{p,\Lambda}(K)$, and $F_\Lambda^{-1}(Q) = f_q^{-1} + \Pi_\Lambda(Q)$. Note that the fermionic self-energy $\Sigma_{p,\Lambda}(K)$ is a matrix in the sublattice labels. Our truncation (4) retains only those vertices which are already present in the bare action (3). Although higher order vertices with more than three external legs are generated by the RG procedure, they are irrelevant at the Gaussian fixed point. In fact, a simple scaling analysis keeping the Gaussian part of $\Gamma_\Lambda[\psi, \phi]$ invariant shows that the renormalized vertices Γ_n with n external legs scale as Λ^{n-3} , implying that all vertices with $n > 3$ external legs are irrelevant. There are five marginal vertices with three external legs, corresponding to the field combinations $\bar{\psi}^A \psi^A \phi$, $\bar{\psi}^B \psi^B \phi$, $\bar{\psi}^A \psi^B \phi$, $\bar{\psi}^B \psi^A \phi$, and $\phi \phi \phi$. While in our cutoff scheme the purely bosonic $\phi \phi \phi$ -vertex does not couple to the flow of the self-energies $\Sigma_p(K)$ and $\Pi(Q)$, the sublattice-changing vertices of the type $\bar{\psi}^A \psi^B \phi$ and $\bar{\psi}^B \psi^A \phi$ are neglected in Eq. (4). We nevertheless believe that our truncation (4) is accurate because the sublattice-preserving vertices of the type $\bar{\psi}^A \psi^A \phi$ and $\bar{\psi}^B \psi^B \phi$ are already finite in the bare action (3).

Within our truncation and cutoff scheme, the self-energies and three-legged vertices appearing in Eq. (4) satisfy the following system of FRG flow equations,

$$\partial_\Lambda \Sigma_p^{ss'}(K) = \int_Q F(Q) \dot{G}_p^{ss'}(K-Q) \Gamma_p^s(K-Q, Q) \Gamma_p^{s'}(K, -Q), \quad (5a)$$

$$\partial_\Lambda \Pi(Q) = \sum_{ss'} \sum_p \int_K \left[\dot{G}_p^{ss'}(K) G_p^{s's}(K-Q) + G_p^{ss'}(K) \dot{G}_p^{s's}(K-Q) \right] \Gamma_p^s(K, -Q) \Gamma_p^{s'}(K-Q, Q), \quad (5b)$$

$$\begin{aligned} \partial_\Lambda \Gamma_p^s(K, Q) = & \sum_{s'} \int_{Q'} F(Q') \left[\dot{G}_p^{ss'}(K+Q-Q') G_p^{s's}(K-Q') + G_p^{ss'}(K+Q-Q') \dot{G}_p^{s's}(K-Q') \right] \\ & \times \Gamma_p^s(K+Q-Q', Q') \Gamma_p^s(K, -Q') \Gamma_p^{s'}(K-Q', Q), \end{aligned} \quad (5c)$$

where for simplicity we have omitted the cutoff label Λ and the single-scale propagator is

$$\dot{G}_{p,\Lambda}(K) = -\delta(k - \Lambda) [i\omega - v_p \boldsymbol{\sigma} \cdot \mathbf{k} - \Sigma_{p,\Lambda}(K)]^{-1}. \quad (6)$$

The derivation of the above FRG equations starting from the general Wetterich equation [8] for the theory defined in Eq. (3) is similar to the derivation of the vertex expansion for mixed Bose-Fermi models discussed in Refs. [6 and 9]. A graphical representation of the flow equations (5a–5c) is shown in Fig. 1. Since we are interested in the low-energy behavior of the Green function, we expand the self-energy to linear order in the frequency,

$$\Sigma_{p,\Lambda}(K) = pV_\Lambda(k) \boldsymbol{\sigma} \cdot \mathbf{k} + (1 - Z_\Lambda^{-1})i\omega + \mathcal{O}(\omega^2). \quad (7)$$

Here Z_Λ is the wave-function renormalization factor. Note that we do not expand the momentum dependence

of the velocity correction $V_\Lambda(k)$. For small frequencies our scale-dependent fermionic propagator is given by

$$G_{p,\Lambda}(K) = -\Theta(k - \Lambda) Z_\Lambda \frac{i\omega + pv_\Lambda(k) \boldsymbol{\sigma} \cdot \mathbf{k}}{\omega^2 + \xi_\Lambda^2(k)}, \quad (8)$$

where $\xi_\Lambda(k) = v_\Lambda(k)k$ is the energy dispersion at cutoff scale Λ and $v_\Lambda(k) = Z_\Lambda[v_F + V_\Lambda(k)]$ is the corresponding velocity. Moreover, we retain only the marginal part $\Gamma_{p,\Lambda}^s(0, 0) \equiv i\gamma_\Lambda$ of the three-point vertices. The flow equation (5a) for the self-energy then reduces to

$$\begin{aligned} \partial_\Lambda \Sigma_{p,\Lambda}(K) = & -\gamma_\Lambda^2 Z_\Lambda \int_{\mathbf{q}, \bar{\omega}} \frac{\delta(q - \Lambda) f_{\mathbf{k}-\mathbf{q}}}{\epsilon_\Lambda(\mathbf{k} - \mathbf{q}, i\omega - i\bar{\omega})} \\ & \times \frac{i\bar{\omega} + pv_\Lambda(q) \boldsymbol{\sigma} \cdot \mathbf{q}}{\bar{\omega}^2 + \xi_\Lambda^2(q)}. \end{aligned} \quad (9)$$

Here we have introduced the cutoff-dependent dielectric

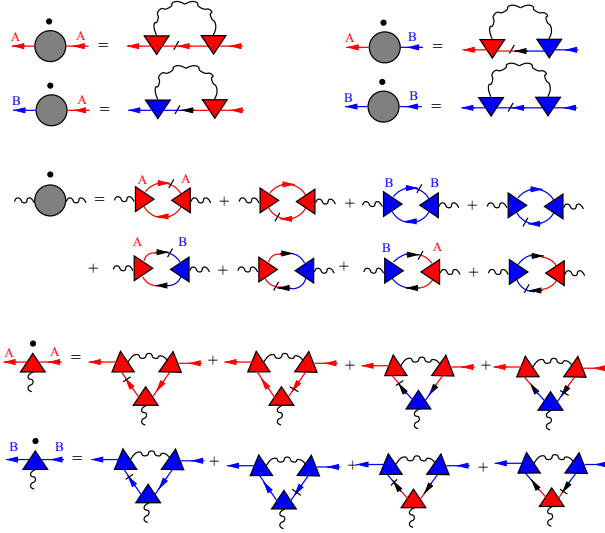


FIG. 1. (Color online) Diagrammatic representation of the FRG flow equations (5a–5c) for the fermionic self-energy (first two lines), for the polarization (third and fourth line), and the three-legged vertices (last two lines). Solid arrows represent the exact cutoff-dependent fermionic propagators, wavy lines represent the corresponding bosonic propagators, and single-scale propagators have an additional slash. The dot over the vertices on the left-hand side represents the derivative with respect to the cutoff Λ . The shaded triangles represent renormalized three-legged vertices with one bosonic and two fermionic external legs carrying the same sublattice label. For clarity, we have marked some of the external legs and the vertices with the associated sublattice labels.

function $\epsilon_\Lambda(Q) = 1 + f_Q \Pi_\Lambda(Q)$. The FRG flow of the polarization is given by

$$\partial_\Lambda \Pi_\Lambda(Q) = -2N_s \gamma_\Lambda^2 Z_\Lambda^2 \int_{\mathbf{k}} \delta(k - \Lambda) \Theta(|\mathbf{k} - \mathbf{q}| - \Lambda) \times \frac{\xi_\Lambda(k) + \xi_\Lambda(|\mathbf{k} - \mathbf{q}|)}{[\xi_\Lambda(k) + \xi_\Lambda(|\mathbf{k} - \mathbf{q}|)]^2 + \bar{\omega}^2} \left[1 - \frac{\mathbf{k} \cdot (\mathbf{k} - \mathbf{q})}{k|\mathbf{k} - \mathbf{q}|} \right], \quad (10)$$

where we have now inserted the spin-degeneracy factor $N_s = 2S + 1 = 2$. It turns out that for $K = Q = 0$ the flow equation (5c) for the three-point vertices $\Gamma_p^s(K, Q)$ reduces to the Ward identity [11] $\gamma_\Lambda Z_\Lambda = 1$, implying a partial cancellation between self-energy and vertex corrections in the above flow equations. Note that this cancellation is not properly taken into account in the random-phase approximation (RPA) where vertex corrections are assumed to be negligible [12]. Nevertheless, by combining the RPA with a RG procedure one can obtain accurate results for the renormalized velocity of graphene [13].

Although it is now straightforward to derive a closed system of FRG flow equations for Z_Λ and the two functions $v_\Lambda(k)$ and $\epsilon_\Lambda(\mathbf{q}, i\bar{\omega})$, let us neglect here the frequency dependence of the dielectric function, $\epsilon_\Lambda(\mathbf{q}, i\bar{\omega}) \approx \epsilon_\Lambda(q)$. In this approximation $Z_\Lambda = \gamma_\Lambda = 1$, but the renormalization of the Fermi velocity is non-perturbatively taken into account. This is sufficient to obtain the correct quantum critical scaling in graphene [10]. After performing one of the integrations in Eqs. (9) and (10) we obtain

$$\Lambda \partial_\Lambda v_\Lambda(k) = -\frac{e^2}{2} \frac{\Lambda}{k} \int_0^\pi \frac{d\varphi}{\pi} \frac{\cos \varphi}{\sqrt{1 - 2(k/\Lambda) \cos \varphi + (k/\Lambda)^2}} \frac{1}{\epsilon_\Lambda(\sqrt{\Lambda^2 - 2k\Lambda \cos \varphi + k^2})}, \quad (11a)$$

$$\Lambda \partial_\Lambda \epsilon_\Lambda(q) = -2N_s e^2 \frac{q}{\Lambda} \int_0^{\pi/2} \frac{d\varphi}{\pi} \frac{\Theta(1 + \frac{q}{2\Lambda} \cos \varphi - \frac{q}{2\Lambda})}{\sqrt{[1 + (q/2\Lambda) \cos \varphi]^2 - [q/2\Lambda]^2}} \frac{\sin^2 \varphi}{[v_\Lambda(\Lambda) + (1 + (q/\Lambda) \cos \varphi) v_\Lambda(\Lambda + q \cos \varphi)]}. \quad (11b)$$

Note that Eq. (11b) has been obtained from Eq. (10) by shifting $\mathbf{k} \rightarrow \mathbf{k} + \mathbf{q}/2$ and then introducing elliptic coordinates. Eqs. (11a) and (11b) form a system of coupled integro-differential equations for the two momentum- and cutoff-dependent functions $v_\Lambda(k)$ and $\epsilon_\Lambda(q)$. The physical renormalized velocity and the static dielectric function are $v(k) = \lim_{\Lambda \rightarrow 0} v_\Lambda(k)$ and $\epsilon(q) = \lim_{\Lambda \rightarrow 0} \epsilon_\Lambda(q)$. We can easily recover the perturbative RG result (1) if we approximate $\epsilon_\Lambda \approx 1$ on the right-hand side of Eq. (11a) and expand the integrand to leading order in k/Λ . However, such an expansion is only valid for $k \ll \Lambda$, so that the physical limit $\Lambda \rightarrow 0$ at fixed $k \neq 0$ is not accessible within this approximation.

We have solved the FRG flow equations (11a, 11b) numerically without further approximations. Note that these equations are non-perturbative in the effective cou-

pling constant $\alpha = e^2/v_F$ and should be quantitatively accurate even for large α . Our numerical result for $v_\Lambda(k)$ in Fig. 2 (a) clearly shows that the external momentum k replaces Λ as effective infrared cutoff as soon as $\Lambda \lesssim k$. The physical momentum-dependent velocity $v(k) = \lim_{\Lambda \rightarrow 0} v_\Lambda(k)$ is shown in Fig. 2 (b). For comparison, we also show the velocities $v_{\Lambda=k}(k)$ and $v_{\Lambda=k}(0)$; the latter can also be obtained using the field-theoretical RG if one stops the RG flow at finite Λ and then substitutes $\Lambda \rightarrow k$. While this recipe works perfectly to leading order in α where the perturbative result for $v(k)$ can be obtained by replacing $\Lambda \rightarrow k$ in Eq. (1), we see from Fig. 2 (b) that this procedure remains approximately valid also for the physically relevant $\alpha = 2.2$. Our FRG result for $v(k)$ can be fitted by $v(k)/v_F = A(\alpha) + B(\alpha) \ln(\Lambda_0/k)$, where $A(2.2) = 1.37$ and $B(2.2) = 0.51$ for $\alpha = 2.2$.

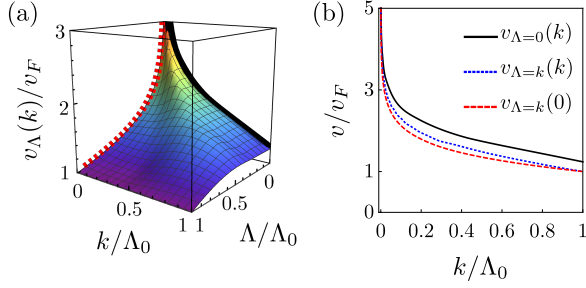


FIG. 2. (Color online) (a) Velocity $v_{\Lambda}(k)$ as a function of infrared cutoff Λ and external momentum k obtained from the numerical solution of Eqs. (11a) and (11b). In (b) the solid line represents our FRG result for the physical momentum-dependent velocity $v(k) = v_{\Lambda=0}(k)$ as a function of k/Λ_0 . For comparison, we also show $v_{\Lambda=k}(0)$ and $v_{\Lambda=k}(k)$.

Note that our result for $B(2.2)$ is very close to the first order expression $\alpha/4 = 0.55$. This is surprising, because in a perturbative expansion the second order correction leads to an additional contribution $b_2\alpha^2$ to the prefactor of $\ln(\Lambda_0/k)$, where according to Mishchenko [16] $b_2 \approx -0.14$, Vafeck *et al.* [15] obtained $b_2 \approx -0.3$, and Barnes *et al.* [14] found $b_2 \approx -0.32$. In any case, for $\alpha = 2.2$ the second order correction is substantial; our FRG calculation suggests that in this case the terms of order α^2 are to a large extent cancelled by higher order corrections.

To compare our results with the experimental data for the renormalized velocity in suspended graphene [2], we need to fix the value of the ultraviolet cutoff Λ_0 which appears as a free parameter in our low-energy action (3). Following the usual field-theoretical procedure [17], we eliminate Λ_0 in favour of some measurable observable. Note that the authors of Ref. [2] use cyclotron resonance to measure the quasi-particle velocity $v(k_F)$ at the Fermi momentum k_F for different densities $n = k_F^2/\pi$ in slightly doped graphene. Assuming that the function $v(k)$ is approximately independent of n (which seems to be reasonable at low densities), we may fix Λ_0 by demanding that our result for $v(k = k_F)$ agrees with the measured quasi-particle velocity at one particular value of k_F . Here we choose the data point at $n \approx 49 \times 10^{10} \text{cm}^{-2}$ to fix Λ_0 ; other choices lead to fits of similar quality. In Fig. 3 we compare the renormalized velocity obtained with this prescription with the experimental data [2]. Obviously, in the entire range of available densities our FRG result agrees quite well with the data.

Finally, in Fig. 4 (a) we show our numerical results for the momentum- and cutoff-dependent dielectric function $\epsilon_{\Lambda}(q)$. Here the external momentum q and the cutoff Λ do not play the same role, because the dielectric function is defined in terms of the bosonic self-energy $\Pi_{\Lambda}(Q)$ while the infrared cutoff has been introduced in the fermionic propagator. The physical dielectric func-

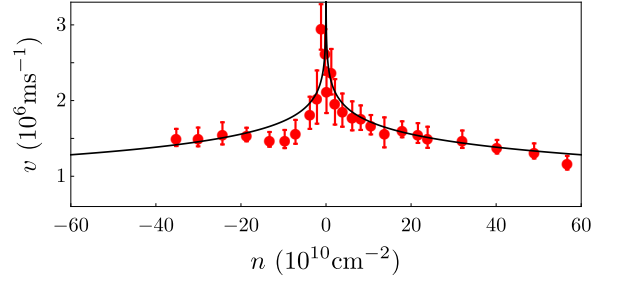


FIG. 3. (Color online) Comparison of our FRG result for the renormalized velocity $v(k_F)$ as a function of the density $n = k_F^2/\pi$ with the data from Ref. [2] (dots with error-bars). The ultraviolet cutoff Λ_0 is fixed as described in the text.

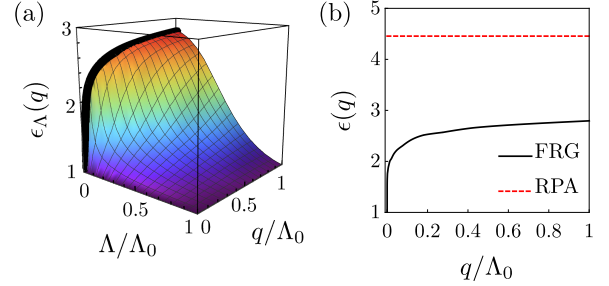


FIG. 4. (Color online) (a) Momentum- and cutoff-dependent dielectric function $\epsilon_{\Lambda}(q)$ obtained from the numerical solution of the FRG flow equations (11a) and (11b). (b) Physical dielectric function $\epsilon(q) = \lim_{\Lambda \rightarrow 0} \epsilon_{\Lambda}(q)$. The dashed line represents the RPA result for $\Lambda_0 \rightarrow \infty$.

tion $\epsilon(q) = \epsilon_{\Lambda=0}(q)$ is shown in Fig. 4 (b). Note that the logarithmic divergence of the velocity $v(k)$ for small k leads to the logarithmic vanishing of the static bosonic self-energy $\Pi(q)$, so that the corresponding dielectric function $\epsilon(q)$ logarithmically approaches unity for $q \rightarrow 0$. Hence, in the static long-wavelength limit the Coulomb interaction in suspended graphene is not screened at all. On the other hand, if we replace the flowing velocity by the bare velocity on the right-hand side of our flow equation (11b) and take the limit $\Lambda_0 \rightarrow \infty$ we recover the RPA result $\epsilon_{\text{RPA}}(q) = 1 + \pi N_s \alpha/4$.

In summary, we have derived and solved non-perturbative FRG flow equations for the momentum- and cutoff-dependent quasi-particle velocity $v_{\Lambda}(k)$ and the static dielectric function $\epsilon_{\Lambda}(q)$ of suspended graphene. In the physical limit $\Lambda \rightarrow 0$ our result for $v(k)$ diverges as $\ln(\Lambda_0/k)$ for $k \rightarrow 0$ and agrees very well with a recent experiment [2]. The dielectric function $\epsilon(q)$ is shown to approach unity for $q \rightarrow 0$, in contrast to the prediction of the RPA. Our approach can be extended in several directions: with some extra numerical effort, the frequency-dependence of the dielectric function can be taken into account. Moreover, we can generalize our approach to allow for the spontaneous formation of a charge-density

wave which transforms the system into an excitonic insulator [1, 18].

We thank A. Geim for making the data for the renormalized velocity from Ref. [2] available to us. Two of us (C. B. and P. K.) acknowledge the hospitality of the physics department of the University of Florida, Gainesville, where part of this work has been carried out.

-
- [1] V. N. Kotov, B. Uchoa, V. M. Pereira, F. Guinea, and A. H. Castro Neto, *Rev. Mod. Phys.* **84**, 1067 (2012).
 - [2] D. C. Elias, R. V. Gorbachev, A. S. Mayorov, S. V. Morozov, A. A. Zhukov, P. Blake, L. A. Ponomarenko, I. V. Grigorieva, K. S. Novoselov, F. Guinea, and A. K. Geim, *Nat. Phys.* **7**, 701 (2011).
 - [3] D. A. Siegel, C. H. Park, C. Hwang, J. Deslippe, A. V. Fedorov, S. G. Louie, and A. Lanzara, *Proc. Natl. Acad. Sci. U.S.A.* **108**, 11365 (2011).
 - [4] G. L. Yu, R. Jalil, B. Belle, A. S. Mayorov, P. Blake, F. Schedin, S. V. Morozov, L. A. Ponomarenko, F. Chiappini, S. Wiedmann, U. Zeitler, M. I. Katsnelson, A. K. Geim, K. S. Novoselov, and D. C. Elias, *Proc. Natl. Acad. Sci. U.S.A.* **110**, 3282 (2013).
 - [5] J. Gonzalez, F. Guinea, and M. A. H. Vozmediano, *Nucl. Phys. B* **424**, 595 (1994).
 - [6] P. Kopietz, L. Bartosch, and F. Schütz, *Introduction to the Functional Renormalization Group* (Springer, Berlin, 2010).
 - [7] W. Metzner, M. Salmhofer, C. Honerkamp, V. Meden, and K. Schönhammer, *Rev. Mod. Phys.* **84**, 299 (2012).
 - [8] C. Wetterich, *Phys. Lett. B* **301**, 90 (1993).
 - [9] F. Schütz, L. Bartosch, and P. Kopietz, *Phys. Rev. B* **72**, 035107 (2005).
 - [10] D. Sheehy and J. Schmalian, *Phys. Rev. Lett.* **99**, 226803 (2007).
 - [11] J. Gonzalez, *Phys. Rev. B* **82**, 155404 (2010).
 - [12] V. N. Kotov, B. Uchoa, and A. H. Castro Neto, *Phys. Rev. B* **78**, 035119 (2008).
 - [13] J. Hofmann, E. Barnes, and S. Das Sarma, *Phys. Rev. Lett.* **113**, 105502 (2014).
 - [14] E. Barnes, E. H. Hwang, R. E. Throckmorton, and S. Das Sarma, *Phys. Rev. B* **89**, 235431 (2014).
 - [15] O. Vafeek and M. J. Case, *Phys. Rev. B* **77**, 033410 (2008).
 - [16] E. G. Mishchenko, *Phys. Rev. Lett.* **98**, 216801 (2007).
 - [17] F. de Juan, A. G. Grushin, and M. A. H. Vozmediano, *Phys. Rev. B* **82**, 125409 (2010).
 - [18] D. V. Khveshchenko, *Phys. Rev. Lett.* **87**, 246802 (2001).